THE PLANT CELL

The Plant Cell, 2025, **37**, koaf084

https://doi.org/10.1093/plcell/koaf084
Advance access publication 11 April 2025
Breakthrough Report

Small DNA elements can act as both insulators and silencers in plants

Tobias Jores,[1,2,3,*] Nicholas A. Mueth,[1] Jackson Tonnies,[1,4,†] Si Nian Char,[5] Bo Liu,[5] Valentina Grillo-Alvarado,[1,6] Shane Abbitt,[7] Ajith Anand,[7,‡] Stéphane Deschamps,[7] Scott Diehn,[7] Bill Gordon-Kamm,[7] Shuping Jiao,[7] Kathy Munkvold,[7,§] Heather Snowgren,[7] Nagesh Sardesai,[7] Stanley Fields,[1,8] Bing Yang,[5,9] Josh T. Cuperus,[1,10] Christine Queitsch[1,10,*]

[1]Department of Genome Sciences, University of Washington, Seattle, WA 98195, USA
[2]Institute of Synthetic Biology, Heinrich-Heine-University Düsseldorf, 40225 Düsseldorf, Germany
[3]CEPLAS—Cluster of Excellence on Plant Sciences, 40225 Düsseldorf, Germany
[4]Graduate Program in Biology, University of Washington, Seattle, WA 98195, USA
[5]Division of Plant Science and Technology, Bond Life Sciences Center, University of Missouri, Columbia, MO 65211, USA
[6]Molecular & Cellular Biology Graduate Program, University of Washington, Seattle, WA 98195, USA
[7]Corteva Agriscience, Johnston, IA 50131, USA
[8]Department of Medicine, University of Washington, Seattle, WA 98195, USA
[9]Donald Danforth Plant Science Center, St. Louis, MO 63132, USA
[10]Brotman Baty Institute for Precision Medicine, University of Washington, Seattle, WA 98195, USA
*Author for correspondence: tobias.jores@hhu.de (T.J.), queitsch@uw.edu (C.Q.)
†Present address: Sound Agriculture, Emeryville, CA, USA
‡Present address: Connect Labs Sacramento, Wexford Science and Technology, Sacramento, CA, USA
§Present address: Foundation for Food & Agriculture Research, Washington, DC, USA
The authors responsible for distribution of materials integral to the findings presented in this article in accordance with the policy described in the Instructions for Authors (https://academic.oup.com/plcell/pages/General-Instructions) are Tobias Jores (tobias.jores@hhu.de) and Christine Queitsch (queitsch@uw.edu).

Abstract

Insulators are *cis*-regulatory elements that separate transcriptional units, whereas silencers are elements that repress transcription regardless of their position. In plants, these elements remain largely uncharacterized. Here, we use the massively parallel reporter assay Plant STARR-seq with short fragments of 8 large insulators to identify more than 100 fragments that block enhancer activity. The short fragments can be combined to generate more powerful insulators that abolish the capacity of the strong viral 35S enhancer to activate the 35S minimal promoter. Unexpectedly, when tested upstream of weak enhancers, these fragments act as silencers and repress transcription. Thus, these elements are capable of insulating or repressing transcription, depending on the regulatory context. We validate our findings in stable transgenic *Arabidopsis thaliana*, maize (*Zea mays*), and rice (*Oryza sativa*) plants. The short elements identified here should be useful building blocks for plant biotechnology.

Introduction

Precise control of gene expression is crucial for plants to grow and develop in a changing environment. Genomic approaches to study plant gene regulation have focused mainly on promoters and enhancers (Weising and Kahl 1991; Ricci et al. 2019; Jores et al. 2020, 2021, 2023; Cuperus 2022; Schmitz et al. 2022). In contrast, repressive elements such as silencers and insulators have received far less attention. Insulators compartmentalize genomes into discrete transcriptional units (Chetverina et al. 2014). Insulators have 1 or both of 2 principal functions (Heger and Wiehe 2014): They block enhancers from interacting with core promoters (enhancer-blocking insulators), or they form barriers against the spread of repressive heterochromatin (barrier insulators). Enhancer-blocking insulators are defined by their ability to act when situated between an enhancer and promoter, but not when the order is reversed such that the enhancer is closer to the promoter than the insulator (Chetverina et al. 2014). Insulators are thought to prevent ectopic gene expression, maintain chromatin accessibility, and enable differentially regulated genes to reside in close proximity to one another (Burgess-Beusse et al. 2002).

To date, most research on insulators has been performed in animal models (Vogelmann et al. 2011). In contrast, only a handful of plant sequences have been shown to act as insulators in transient or stable transgenic plant reporter assays (Singer et al. 2012; Kurbidaeva and Purugganan 2021). For example, the transformation booster sequence (TBS) from *Petunia hybrida*, the β-phaseolin gene from *Phaseolus vulgaris*, and a *gypsy*-like sequence from Arabidopsis (*Arabidopsis thaliana*) function as enhancer-blocking insulators in transgenic plants (van der Geest and Hall 1997; Hily et al. 2009; Singer and Cox 2013). In addition, a few heterologous sequences show enhancer-blocking insulator activity in plants, including λ-EXOB from phage λ, BEAD-1C from humans, and UASrpg from yeast (Gudynaite-Savitch et al. 2009; Singer et al. 2009). In these studies, insulator activity was inferred from GUS staining or fluorescence of a reporter gene, both measures

Received February 10, 2025. Accepted March 16, 2025.

with limitations of dynamic range, quantification accuracy, and throughput.

Because the enhancer-blocking activity of insulators is detected as reduced transcription in the commonly used reporter assays, care must be taken to distinguish between insulators and silencers, which could also cause reduced transcription in these assays. Silencers recruit repressive transcription factors and, like enhancers, can act in a position-independent manner (i.e. upstream or downstream of an enhancer) (Laimins et al. 1986; Ogbourne and Antalis 1998; Gisselbrecht et al. 2020; Pang and Snyder 2020; Schmitz et al. 2022). This position-independency is thought to be a key difference between silencers and insulators that differentiates between the 2 element types.

To date, no general principles are known that typify insulator or silencer function in plants nor are there high-throughput methods to identify these elements. Short and strong insulators will facilitate synthetic biology applications to ensure predictable expression of transgenes, blocking inappropriate enhancer–promoter interactions and alleviating chromatin position effects (Singer et al. 2012). Similarly, silencers will enable fine-tuning of transgene expression and minimize expression noise. Furthermore, understanding the sequence features of functional plant insulators and silencers will allow targeting similar elements in plant genomes to engineer gene expression.

Here, we applied Plant STARR-seq, a massively parallel reporter assay, to test the insulator and silencer activity of over 100 short (170 bp) fragments derived from either previously described enhancer-blocking insulators or 2 synthetic insulator sequences. Our assay distinguishes enhancer-blocking activity from transcriptional repression and reveals that the insulator-derived elements harbor both insulator-like and silencer-like activities. Promising elements were tested and verified in stable transgenic Arabidopsis, rice, and maize plants.

Results

Plant STARR-seq detects the activity of enhancer-blocking insulators

We recently developed Plant STARR-seq, a versatile massively parallel reporter assay that can identify and characterize diverse *cis*-regulatory elements (Jores et al. 2020, 2021, 2023, 2024; Gorjifard et al. 2024). For the Plant STARR-seq assay, up to hundreds of thousands of candidate sequences are cloned in the position of the respective regulatory element to be tested within a suitable reporter construct. For example, they can be tested as promoters, enhancers, terminators, or, as done here, as insulators or silencers. The candidate sequences are linked to short barcodes located in the open reading frame of a reporter gene. Pooled libraries of reporter constructs are used for transient transformation of *Nicotiana benthamiana* leaves or maize protoplasts; other transient expression systems are also possible (Voichek et al. 2024). After an incubation period, the mRNA of the reporter gene is extracted, and the relative abundance of the barcode sequences in the input DNA and the extracted RNA is determined by next-generation sequencing. Since regulatory elements affect transcription levels (or RNA stability), the enrichment or depletion of a linked barcode in the RNA relative to its DNA input is a measure of an element's ability to increase or decrease transcription (or RNA stability).

To test whether Plant STARR-seq can identify enhancer-blocking insulators, we created a reporter construct consisting of a barcoded green fluorescent protein (GFP) gene under the control of a 35S minimal promoter (−46 to +5 relative to the 35S transcription start site) coupled to a 35S enhancer; insulator candidates were placed between this enhancer and promoter (Supplementary Fig. S1A). We selected 4 heterologous sequences that show insulator activity in plants (λ-EXOB, BEAD-1C, UASrpg, and a *Drosophila* gypsy element) (Gudynaite-Savitch et al. 2009; Singer et al. 2009, 2012; She et al. 2010), and 2 synthetic sequences (sIns1 and sIns2) for which preliminary data suggested they might act as insulators. The synthetic sequences sIns1 and sIns2 derive from a plasmid backbone and a human codon-optimized coding sequence of Cas9, respectively. The insulator candidate sequences were cloned in the forward or reverse orientation, and their insulator activity was determined by Plant STARR-seq in *N. benthamiana* leaves and maize (*Zea mays*) protoplasts. Constructs without the 35S enhancer and without an insulator (noEnh) or with the 35S enhancer and without an insulator (noIns) were included as controls (Supplementary Fig. S1B). We measured insulator activity as reduced enrichment compared with the enrichment of the no insulator (noIns) control. Except for the gypsy element, the other 5 tested insulator candidates resulted in reduced enrichment, indicating that they function as enhancer-blocking insulators in this assay (Supplementary Fig. S1C). For some of the insulators, we observed orientation-dependent activity (Supplementary Fig. S1C). The gypsy element shows enhancer-blocking and barrier insulator activities in *Drosophila* (Gdula et al. 1996); however, it lacks enhancer-blocking activity in plants (She et al. 2010), consistent with our results (Supplementary Fig. S1C). The finding that the gypsy element does not affect reporter gene expression suggests that the effects seen with the other insulator candidates are not caused merely by the increased distance between the minimal promoter and enhancer but are a result of sequence-specific insulator activity. Taken together, we demonstrate that Plant STARR-seq reproducibly (Supplementary Fig. S2) measures insulator activity.

The large size of known enhancer-blocking insulators precludes their application in plant biotechnology (Singer et al. 2012). To identify short sequences with insulator activity, we array-synthesized overlapping 170 bp fragments of each of the 6 insulators in addition to 2 plant sequences with insulator activity (β-phaseolin and TBS), and measured the enhancer-blocking activity of these fragments (Fig. 1A). Many fragments retained partial insulator activity in *N. benthamiana* and maize (Fig. 1B and Supplementary Data Set 1), but their activity varied between the 2 assay systems, pointing to species-specific differences (Fig. 1C).

Overall, 7 of the 8 insulators, excluding only the gypsy element, harbored clusters of fragments that partially blocked the 35S enhancer (Fig. 1D). This clustering of active fragments is likely driven by local nucleotide composition because GC content is strongly correlated (R^2 of 0.54 and 0.26 in *N. benthamiana* and maize, respectively) with a fragment's insulator activity (Fig. 1E). The lower correlation of GC content and insulator activity observed in maize likely reflects the maize genome's higher GC content. Similar tendencies were previously observed for promoter and terminator activities (Jores et al. 2021; Gorjifard et al. 2024). However, GC content does not fully explain insulator activity: Many insulator-derived fragments showed orientation-dependent activity (Fig. 1D). Furthermore, we tested the insulator-derived fragments with the *AB80* enhancer from *Pisum sativum* and *Cab-1* enhancer from *Triticum aestivum*, which drive the expression of chlorophyll *a-b* binding proteins, and found that the activity of these fragments was largely enhancer-independent (Fig. 1, B and F).

To validate our findings, we measured insulator activity in stable transgenic plants (Fig. 2). Full-length insulators and fragments thereof showed enhancer-blocking insulator activity in

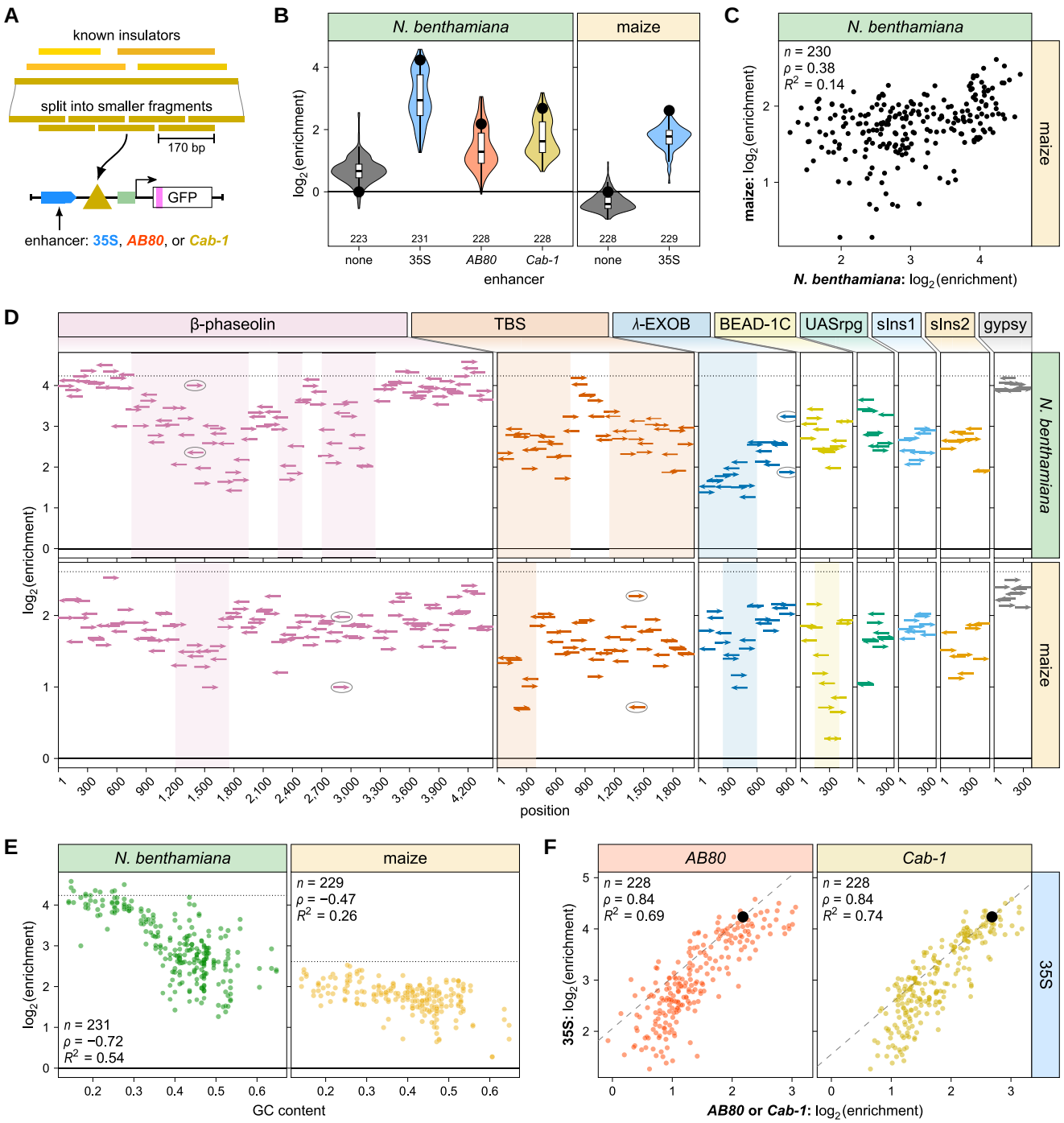

Figure 1. Short fragments exhibit enhancer-blocking insulator activity. **A)** Known insulators were split into partially overlapping 170-bp fragments. The insulator fragments were cloned in the forward or reverse orientation between a 35S, *AB80*, or *Cab-1* enhancer and a 35S minimal promoter (green rectangle) driving the expression of a barcoded GFP reporter gene. Constructs without an enhancer (none) but with insulator fragments were also created. **B)** All insulator fragment constructs were pooled and subjected to Plant STARR-seq in *N. benthamiana* leaves (*N. benthamiana*) and maize protoplasts (maize). Reporter mRNA enrichment was normalized to a control construct without an enhancer or insulator (noEnh; $\log_2$ set to 0). The enrichment of a control construct without an insulator is indicated as a black dot. Violin plots represent the kernel density distribution and the box plots inside represent the median (center line), upper and lower quartiles, and 1.5× interquartile range (whiskers) for all corresponding constructs. Numbers at the bottom of each violin indicate the number of samples in each group. **C)** Correlation between the enrichment of insulator fragments in constructs with the 35S enhancer in *N. benthamiana* leaves and maize protoplasts. **D)** Enrichment of constructs with insulator fragments cloned between the 35S enhancer and minimal promoter. The position along the full-length insulator and the orientation (arrow pointing right, fwd; arrow pointing left, rev) of the fragments is indicated by arrows. Clusters of active fragments are shown as shaded areas. Insulators with highly orientation-dependent activity are circled. **E)** Correlation between insulator fragment enrichment and GC content for constructs with the 35S enhancer. **F)** Correlation between insulator fragment enrichment in *N. benthamiana* leaves in constructs with the indicated enhancers. The dashed line represents a $y = x$ line fitted through the point corresponding to a control construct without an insulator (black dot). Pearson's R^2, Spearman's ρ, and number (n) of constructs are indicated in **(C)**, **(E)**, and **(F)**. The dotted line in **(D)** and **(E)** represents the enrichment of a control construct without an insulator.

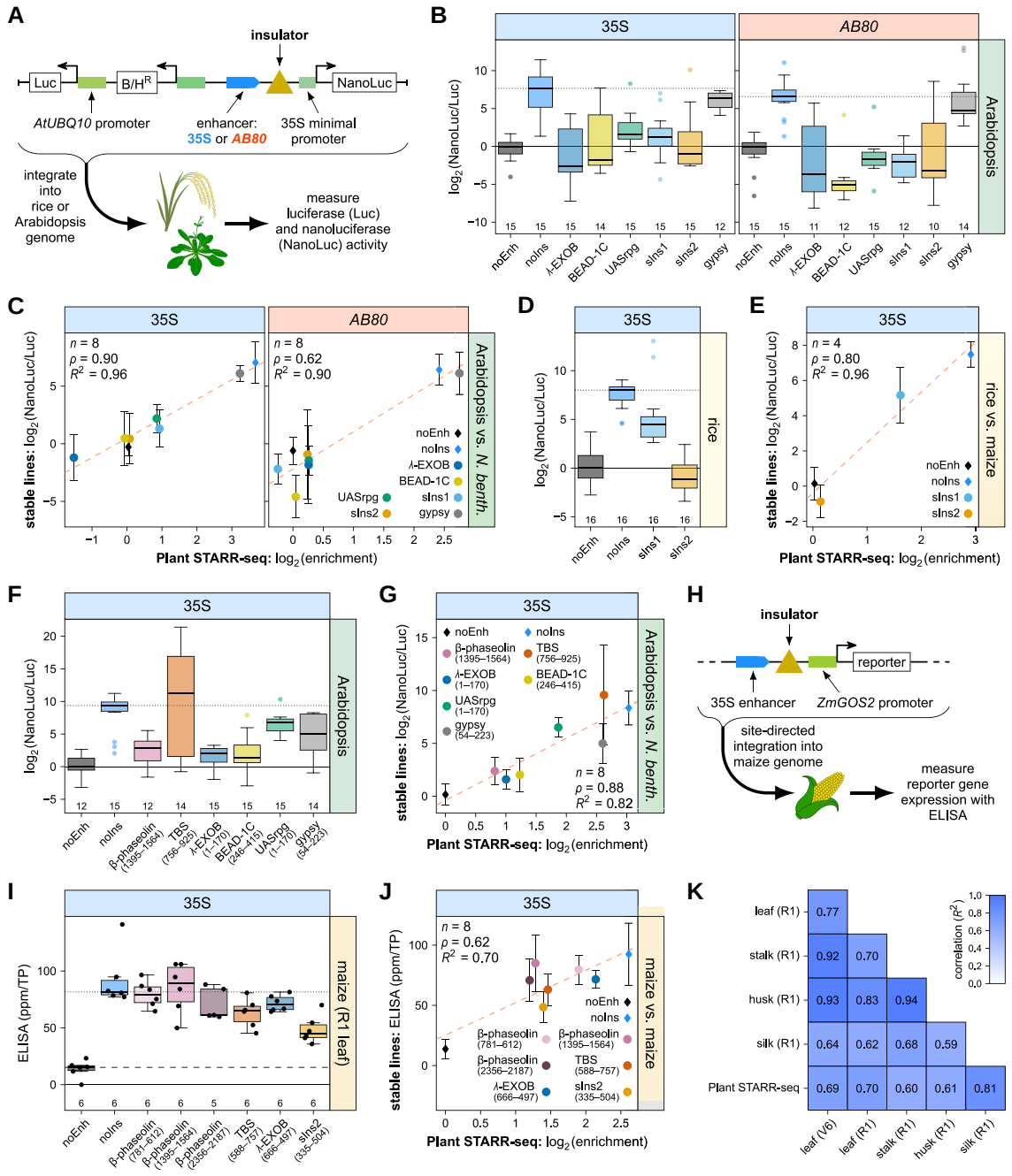

Figure 2. Insulators are active in stable transgenic lines in Arabidopsis, rice, and maize. **A)** Transgenic Arabidopsis and rice lines were generated with T-DNAs harboring a constitutively expressed luciferase (Luc) gene and a nanoluciferase (NanoLuc) gene under control of a 35S minimal promoter coupled to the 35S or *AB80* enhancer (as indicated above the plots) with insulator candidates inserted between the enhancer and promoter. Nanoluciferase activity was measured in at least 4 plants from these lines and normalized to the activity of luciferase. The NanoLuc/Luc ratio was normalized to a control construct without an enhancer or insulator (noEnh; $\log_2$ set to 0). **B** and **C)** The activity of full-length insulators was measured in Arabidopsis lines **(B)** and compared with the corresponding results from Plant STARR-seq in *N. benthamiana* leaves **(C)**. **D** and **E)** The activity of synthetic full-length insulators was measured in rice lines **(D)** and compared with the corresponding results from Plant STARR-seq in maize protoplasts **(E)**. **F** and **G)** The activity of insulator fragments was measured in Arabidopsis lines **(F)** and compared with the corresponding results from Plant STARR-seq in *N. benthamiana* leaves **(G)**. **H)** For transgenic maize lines, a reporter gene driven by the constitutive, moderate-strength *ZmGOS2* promoter and an upstream 35S enhancer was created and insulator fragments were inserted between the enhancer and promoter. The reporter gene cassette was inserted in the maize genome by site-directed integration and the expression of the reporter gene was measured in various tissues/developmental stages by ELISA. **I** and **J)** The activity of insulator fragments was measured in R1 leaves of transgenic maize lines **(I)** and compared with the corresponding results from Plant STARR-seq in maize protoplasts **(J)**. **K)** Correlation (Pearson's R^2) between the expression of all tested constructs across different tissues and developmental stages. The correlation with Plant STARR-seq results from maize protoplasts is also shown. Box plots in **(B)**, **(D)**, **(F)**, and **(I)** represent the median (center line), upper and lower quartiles (box limits), 1.5× interquartile range (whiskers), and outliers (points) for all corresponding samples from 2 to 3 independent replicates. Numbers at the bottom of each box plot indicate the number of samples in each group. For groups with less than 10 samples, individual data points are shown as black dots. In **(C)**, **(E)**, **(G)**, and **(J)**, the dashed line represents a linear regression line and error bars represent the 95% confidence interval. Pearson's *R2*, Spearman's ρ, and number (*n*) of constructs are indicated. The dotted line in **(B)**, **(D)**, **(F)**, and **(I)** represents the median enrichment of a control construct without an insulator, and the dashed line in **(I)** represents the median enrichment of a control construct without an insulator and without the 35S enhancer.

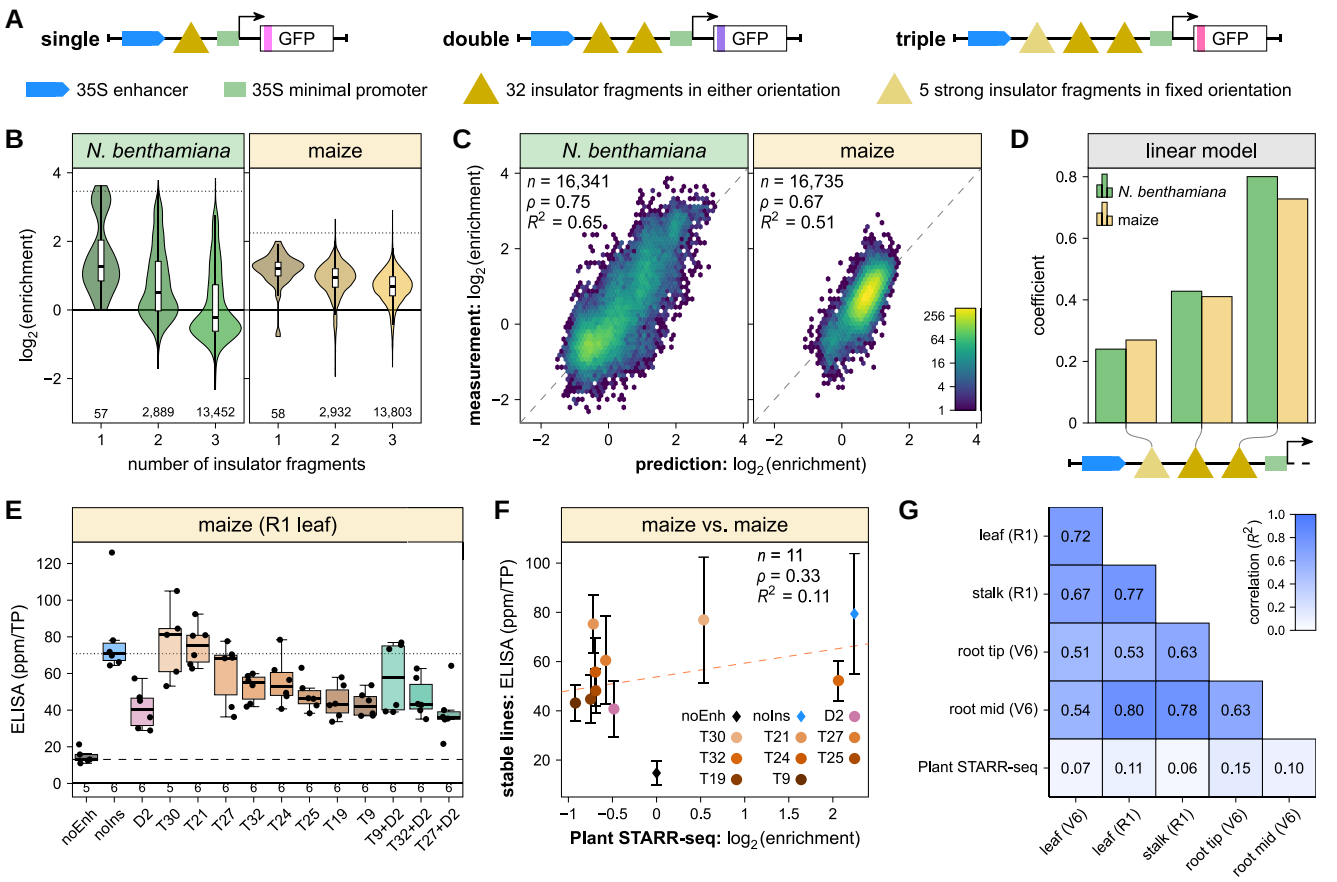

Figure 3. Insulator fragments can be stacked to create very strong enhancer-blocking insulators. **A)** One, 2, or 3 170-bp fragments of known insulators were cloned between a 35S enhancer and a 35S minimal promoter driving the expression of a barcoded GFP reporter gene. **B)** All insulator constructs were pooled and subjected to Plant STARR-seq in *N. benthamiana* leaves (*N. benthamiana*) and maize protoplasts (maize). Reporter mRNA enrichment was normalized to a control construct without an enhancer or insulator ($\log_2$ set to 0). Violin plots are as defined in Fig. 1B. **C)** A linear model was trained to predict the enrichment of stacked insulator constructs based on the activity of individual insulator fragments and their position within the construct. The correlation between the model's prediction (prediction) and experimentally determined enrichment values (measurement) is shown as a hexbin plot (color represents the count of points in each hexagon). Pearson's R^2, Spearman's ρ, and number (n) of fragments are indicated. **D)** Coefficients assigned by the linear model to insulator fragments in the indicated positions of the stacked constructs. **E** and **F)** The activity of insulator fragment combinations in constructs as in Fig. 2H was measured in R1 leaves of transgenic maize lines **(E)** and compared with the corresponding results from Plant STARR-seq in maize protoplasts **(F)**. Box plots are as defined in Fig. 2. The enrichment of a control construct without an insulator (noIns) is indicated as a dotted line. In **(F)**, the dashed line represents a linear regression line and error bars represent the 95% confidence interval. Pearson's R^2, Spearman's ρ, and number (n) of constructs are indicated. **G)** Correlation (Pearson's R^2) between the expression of all tested constructs across different tissues and developmental stages. The correlation with Plant STARR-seq results from maize protoplasts is also shown. The dotted line in **(B)** and **(E)** represents the enrichment of a control construct without an insulator, and the dashed line in **(E)** represents the enrichment of a control construct without an insulator and without the 35S enhancer.

Arabidopsis, rice (*Oryza sativa*), and maize, well correlated with the Plant STARR-seq results (Fig. 2 and Supplementary Fig. S3). In maize, we measured insulator activity in 4 tissues (leaf, stalk, silk, and husk) and 2 developmental stages (V6 and R1) and obtained similar results, indicating that these insulators do not act in a tissue-specific manner (Fig. 2K).

Active fragments can be assembled into strong insulators

We asked whether insulator activity can be increased by combining up to 3 fragments. We selected 26 fragments with high insulator activity (selected from the top 25% of all fragments) in *N. benthamiana* and 6 fragments with low insulator activity (selected from the bottom 25% of all fragments) in *N. benthamiana* (Supplementary Table S1). These fragments were used in the forward and reverse orientation to build constructs with both the individual fragments and with the over 2,900 randomly generated 2-fragment combinations. Additionally, we built over 13,000 three-fragment combinations that added 1 of 5 fragments with very high insulator activity (selected from the top 5% of all fragments; Supplementary Table S1) upstream of the randomly generated 2-fragment combinations. Fragments and fragment combinations were cloned between the 35S enhancer and 35S minimal promoter (Fig. 3A). Increasing the number of insulator fragments increased insulator activity. In *N. benthamiana*, most constructs with 3 insulator fragments completely blocked the 35S enhancer (Fig. 3B and Supplementary Data Set 2). Combinations of fragments derived from different full-length insulators showed a similar activity distribution to combinations of fragments derived from the same full-length insulator. Similarly, the activity distribution of combinations with 2 copies of the same fragment was largely indistinguishable from that of combinations with 2 nonidentical fragments.

We trained a linear model based on the insulator activity of the individual fragments and their position in the construct to predict the insulator activity of 2-fragment and 3-fragment combinations in *N. benthamiana* and maize (Fig. 3C). Model accuracy was similar

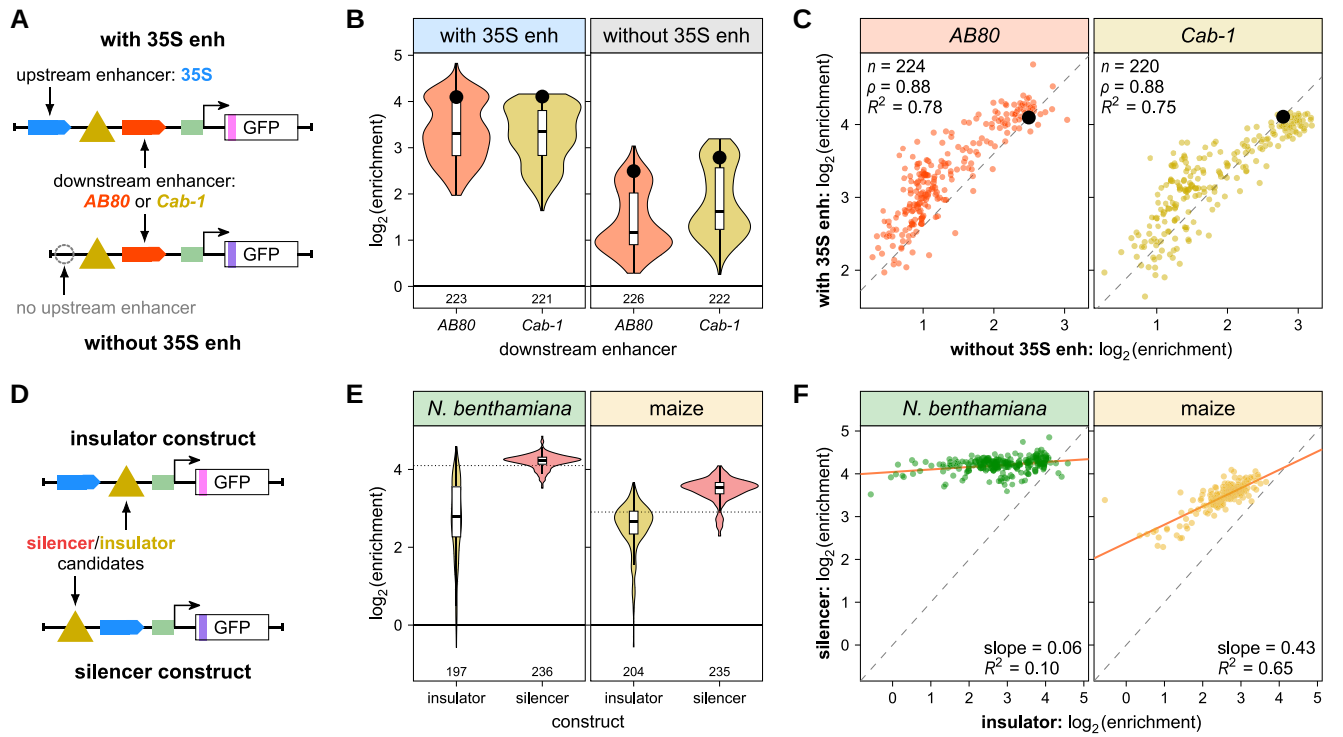

Figure 4. Insulators exhibit silencer activity in some contexts. **A)** Insulator fragments (yellow triangle) were cloned upstream of a *AB80* or *Cab-1* enhancer and a 35S minimal promoter (green rectangle) driving the expression of a barcoded GFP reporter gene. Half of the constructs also harbored a 35S enhancer upstream of the insulator fragments (with 35S) while the other half lacked an upstream enhancer (without 35S). **B)** All constructs were pooled and subjected to Plant STARR-seq in *N. benthamiana* leaves. Reporter mRNA enrichment was normalized to a control construct without an enhancer or insulator (noEnh; $\log_2$ set to 0). The enrichment of a control construct without an insulator is indicated as a black dot. **C)** Correlation between insulator fragment activity in constructs with or without the upstream 35S enhancer. The dashed line represents a $y = x$ line fitted through the point corresponding to a control construct without an insulator (black dot). **D)** Insulator fragments (yellow triangle) were cloned in between (insulator construct) or upstream of (silencer construct) a 35S enhancer (blue arrow) and a 35S minimal promoter (green rectangle) driving the expression of a barcoded GFP reporter gene. **E)** All constructs were pooled and subjected to Plant STARR-seq in *N. benthamiana* leaves (*N. benthamiana*) or maize protoplasts (maize). Reporter mRNA enrichment was normalized to a control construct without an enhancer or insulator (noEnh; $\log_2$ set to 0). The enrichment of a control construct without an insulator is indicated as a dotted line. **F)** Comparison of the enrichment of insulator fragments in insulator or silencer constructs. A linear regression line is shown as a solid line and its slope and goodness-of-fit (R^2) is indicated. Violin plots in **(B)** and **(E)** are as defined in Fig. 1B.

for the 2-fragment and 3-fragment combinations in *N. benthamiana* (R^2 of 0.67 and 0.62, respectively). In maize, prediction accuracy was higher for the 2-fragment combinations than for the 3-fragment combinations (R^2 of 0.60 and 0.48, respectively). The model coefficients showed that the fragment closest to the minimal promoter contributes the most to the combined insulator activity, while the fragment closest to the enhancer contributes the least (Fig. 3D). Taken together, the insulator activity of the individual fragments appears to be the key determinant for the activity of the fragment combinations.

Next, we tested the activity of 1 two-fragment combination and 9 three-fragment combinations (Supplementary Table S2) in stable maize plants. Most of these fragment combinations showed insulator activity in the transgenic maize plants (Fig. 3E and Supplementary Fig. S4A). However, their activity was weaker than observed in the Plant STARR-seq experiments, likely because we used the moderate-strength *ZmGOS2* promoter (Barbour et al. 2003) for the transgenic maize reporter constructs instead of the minimal 35S promoter used in Plant STARR-seq (Fig. 3F and Supplementary Fig. S4B). To further increase insulator activity, we cloned the 2-fragment combination D2 downstream of the 3-fragment combinations T9, T32, and T27 (Supplementary Table S2) to yield 3 constructs of 5 fragments (T9 + D2, T32 + D2, and T27 + D2). These 5-fragment combinations showed similar insulator activity as the corresponding 2- or 3-fragment combinations (Fig. 3E and Supplementary Fig. S4A), indicating diminishing returns from stacking increasing numbers of fragments. Because most insulator combinations reached the detection limit in our Plant STARR-seq assay but not in the stable maize plants, the correlation between the ELISA and Plant STARR-seq data was low (Fig. 3, F and G and Supplementary Fig. S4B). However, we observed a strong correlation between ELISA results for samples obtained from different plant tissues (leaf, stalk, and root) and developmental stages (V6 and R1). This observation is consistent with our results for single insulator fragments and indicates that insulator activity is not strongly affected by tissue identity or developmental stage.

Insulator-derived fragments also exhibit silencer activity

The comparison of the Plant STARR-seq and stable maize data suggests that insulator activity might be promoter-dependent. To investigate this hypothesis, we built constructs with hybrid promoters by inserting the *AB80* or *Cab-1* enhancer between the 35S minimal promoter and the insulator fragments and tested if an additional downstream enhancer affected the ability of the insulator-derived fragments to block an upstream 35S enhancer (Fig. 4A, top). Many fragments showed insulator activity with both downstream enhancers (Fig. 4B, left and Supplementary Data Set 3) and this activity was only slightly weaker than in constructs without a downstream enhancer (Supplementary Fig. S5).

This finding suggests that the insulator-derived fragments remain active at a greater distance and work with more complex promoters than the short 35S minimal promoter.

We also tested a set of control constructs without the upstream 35S enhancer (Fig. 4A, bottom) and found that many insulator fragments resulted in lower enrichment than a control construct without an insulator fragment (Fig. 4B, right and Supplementary Data Set 3), indicating transcriptional repression. The enrichment of reporter constructs with and without the upstream 35S enhancer was well correlated (Fig. 4C). These results demonstrate that fragments derived from characterized insulators with enhancer-blocking activity in Plant-STARR-seq can also function as transcriptional silencers (i.e. they can reduce expression in a position-independent manner).

To rigorously assess whether the insulator-derived fragments had silencer activity, we built a new library with 2 different construct layouts: (i) in the "insulator" construct, the fragments were inserted between the 35S enhancer and 35S minimal promoter; and (ii) in the "silencer" construct, the fragments were inserted upstream of the 35S enhancer (Fig. 4D). Since enhancer-blocking insulators need to reside between promoters and enhancers to interfere with their interaction, their blocking activity can only be detected in the insulator construct. In contrast, the activity of silencers is position-independent and can be observed in both constructs. Therefore, the comparison of the activity of a given fragment in both constructs is required to detect and distinguish insulator and silencer activities. As before, many fragments led to a reduced enrichment of the reporter gene when inserted between the enhancer and promoter (i.e. in the insulator construct). The insulator-derived fragments showed little to no activity in the silencer construct in *N. benthamiana*; however, we observed some silencer activity in maize (Fig. 4E and Supplementary Data Set 4).

We reasoned that the activity of fragments in the insulator construct might be a combination of enhancer-blocking and silencer activity. To quantify what fraction of the apparent insulator activity could be explained by transcriptional repression rather than insulation, we plotted the activities of all fragments in the insulator construct against their activities in the silencer construct (Fig. 4F). The slope of the regression line in these plots is a proxy for the maximal contribution of transcriptional repression to the apparent insulator activity. Up to 6% and 43% of the observed activity in the insulator construct could be explained by silencer activity in *N. benthamiana* and maize, respectively (Fig. 4F).

Silencer activity depends on enhancer strength

Because we found evidence of silencer activity in *N. benthamiana* leaves in constructs containing the *AB80* or *Cab-1* enhancer (Fig. 4, B and C), but not in those with the strong 35S enhancer (Fig. 4, E and F), we built insulator and silencer constructs with 8 different enhancers (Fig. 5, A and B). These enhancers showed a wide range of strength in *N. benthamiana* but were all, apart from the 35S enhancer, weak in maize (Fig. 5B).

We tested these enhancers with 6 full-length insulators and 6 insulator-derived fragments (Supplementary Table S3). Insulators and insulator fragments showed little activity as silencers with strong enhancers (like the 35S, At-9661, and Sl-12881 enhancers in *N. benthamiana* and the 35S enhancer in maize) but much more activity as silencers with weak enhancers (Fig. 5C and Supplementary Data Set 5). We did not find any fragments that show high activity in the silencer construct but not in the insulator construct. Similarly, all fragments with high activity in the insulator construct also show high activity in silencer constructs with weak enhancers. Overall, we observe a strong correlation (R^2 of 0.35 to 0.97) between the activities of the tested fragments in the insulator and silencer constructs regardless of the strength of the enhancer used in these constructs. These results conclusively demonstrate that these previously identified insulators and their fragments can function as enhancer-blocking insulators and as silencers depending on regulatory context.

As before, we plotted the enrichment of fragments in insulator constructs against their enrichment in silencer constructs. We used the slope of a linear regression line as a proxy to determine how much of the apparent insulator activity could be explained by silencer activity. For constructs with strong enhancers, between 6% and 27% of the apparent insulator activity could be explained by silencer activity. This proportion increased with weak enhancers, such that silencer activity could explain up to 94% of the observed activity in the insulator construct. Overall, the slopes negatively correlated with the strength of the corresponding enhancer (Fig. 5D).

To test whether the insulators showed silencer activity when integrated into the genome, we used dual-luciferase reporter constructs with the insulator residing upstream of the 35S or *AB80* enhancer to generate stable transgenic Arabidopsis plants (Supplementary Fig. S6A). As in the transient Plant STARR-seq experiments, the insulators showed no silencer activity with the strong 35S enhancer and partial silencer activity with the somewhat weaker *AB80* enhancer in transgenic Arabidopsis plants (Supplementary Fig. S6, B to D). Taken together, these results are consistent with the observation that previously identified insulators show silencer activity that is inversely correlated with the strength of the enhancer with which they are paired.

Discussion

Using the high-throughput Plant STARR-seq assay on fragments of insulators known to be functional in plants, we identified more than 100 different 170-bp fragments with enhancer-blocking activity. These short fragments could be combined to generate stronger insulators, some capable of completely blocking the activity of the viral 35S enhancer. The fragments were active as insulators with different enhancers and promoters across diverse plant tissues. Additionally, these insulators and their fragments showed silencer activity when coupled with weak enhancers.

Taken together, these observations reveal a striking case of context-dependent *cis*-regulatory activity, where the activity of 1 *cis*-regulatory element (the insulator fragment) quantitatively depends on the strength of a second *cis*-regulatory element (the enhancer). Consistent with other work, this finding showcases the complexity of regulatory grammar, wherein *cis*-regulatory elements can have multiple activities that may be observed only in specific conditions or contexts (Schmitz et al. 2022). For example, mesoderm-specific *Drosophila* silencers often function as enhancers in other cell types (Gisselbrecht et al. 2020). Thus, regulatory elements must be tested systematically in different contexts—e.g. as insulators, silencers, or enhancers, and across species and tissues—to understand the mechanistic underpinnings of their potentially complex functions.

The elements studied here behaved like classical enhancer-blocking insulators in combination with strong enhancers, as they reduced reporter expression only when inserted between the enhancer and promoter. In contrast, with weak enhancers, the same elements behaved like typical silencers that repressed

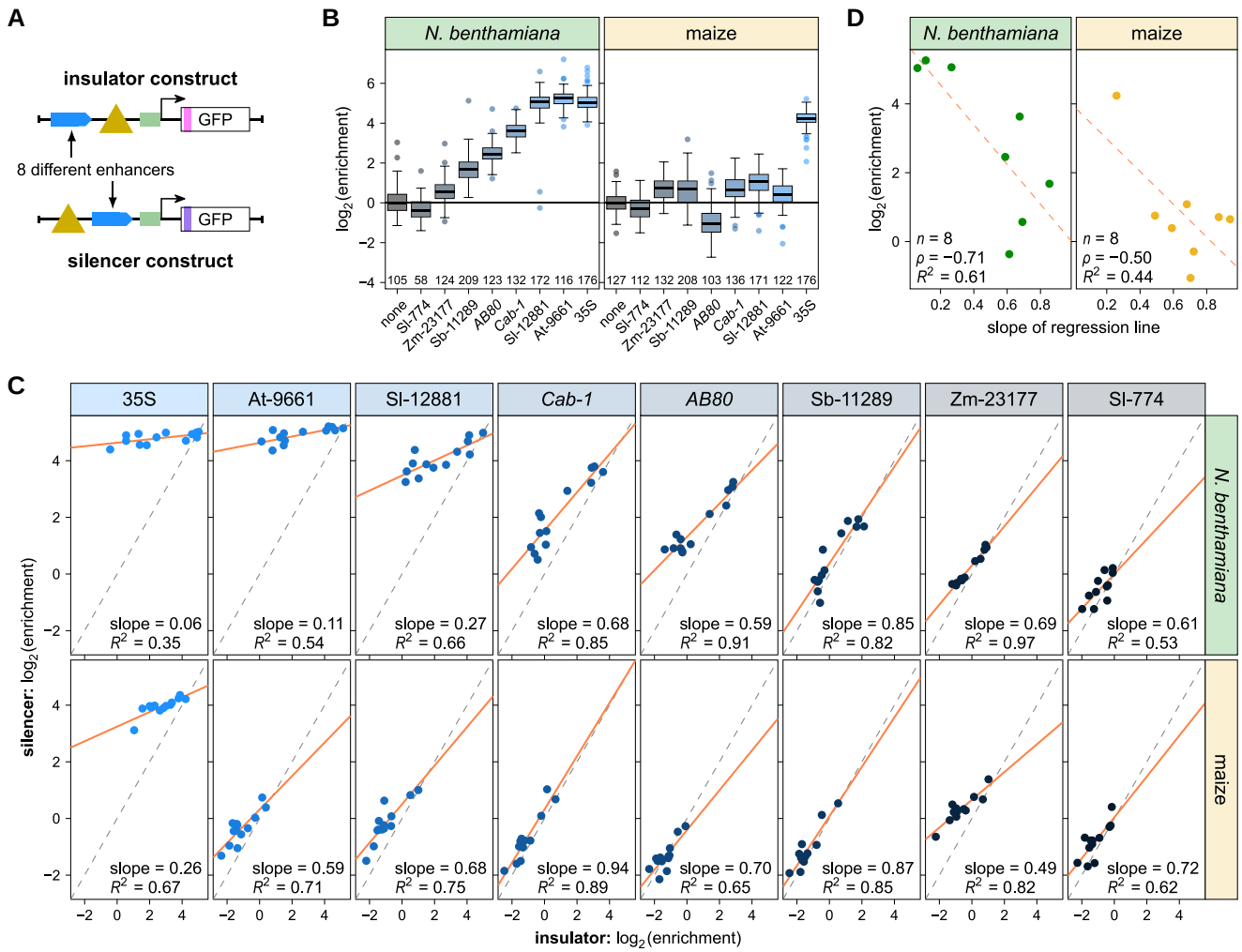

Figure 5. Silencer activity depends on enhancer strength. **A)** Selected insulators and insulator fragments (yellow triangle) were cloned in between (insulator construct) or upstream of (silencer construct) an enhancer and a 35S minimal promoter (green rectangle) driving the expression of a barcoded GFP reporter gene. Eight different enhancers were used to build these constructs. All constructs were pooled and subjected to Plant STARR-seq in *N. benthamiana* leaves (*N. benthamiana*) or maize protoplasts (maize). **B)** Strength of the 8 enhancers in constructs without an insulator. Reporter mRNA enrichment was normalized to a control construct without an enhancer (none; $\log_2$ set to 0). Box plots represent the median (center line), upper and lower quartiles, and 1.5× interquartile range (whiskers) for all corresponding barcodes from 2 independent replicates. Numbers at the bottom of the plot indicate the number of samples in each group. **C)** Comparison of the enrichment of insulators and insulator fragments in insulator or silencer constructs. A linear regression line is shown as a solid line and its slope and goodness-of-fit (R^2) is indicated. **D)** Correlation between the slope of the regression lines from **(C)** and the strength of the corresponding enhancer from **(B)**. Pearson's R^2, Spearman's ρ, and number (n) of constructs are indicated. A linear regression line is shown as a dashed line.

transcription in a position-independent manner. With intermediate strength enhancers, a continuum between these 2 extremes was observed: The elements reduced transcription when placed either upstream or downstream of the enhancer, but the effect was stronger in the downstream context. It remains to be determined if the observed activity is a combination of distinct insulator and silencer functions or if we identified an unknown regulatory mechanism. Our observation that, independent of enhancer strength, the activity of fragments in insulator and silencer constructs is well correlated suggests that the latter might be the case.

One question not addressed in this study is whether the enhancer-blocking elements identified here can also act as barrier insulators (i.e. block the spread of repressive heterochromatin). As evidenced by the lack of activity of the gypsy element, a known barrier insulator in plants (She et al. 2010), our assay cannot detect barrier insulator function. Work in animal systems led to the discovery of sequences with both enhancer-blocking and barrier functions, although at least in some cases this can be explained through the co-occurrence of separable enhancer-blocking and barrier elements (Gdula et al. 1996; Recillas-Targa et al. 2002; Gaszner and Felsenfeld 2006). In plants, further work will be required to test if elements can act as both enhancer-blocking and barrier insulators or if these functions require different sequence or structure elements altogether.

To date, the molecular mechanisms underlying plant insulator function are unknown. In animals, several DNA-binding proteins, including su(Hw), BEAF-32, and Zw5 in *Drosophila* (Parkhurst et al. 1988; Zhao et al. 1995; Gaszner et al. 1999) and CTCF in humans (Bell et al. 1999), play a role in insulator function. However, homologs of these proteins have not been identified in plants. The number of fragments with insulator activity tested here is too small to derive putative protein-binding motifs with confidence. Moreover, there is no evidence that insulation in plants requires protein

binding. In contrast to enhancer activity (Banerji et al. 1981; Schmitz et al. 2022), we found that insulator activity was orientation-dependent, as has been observed in animals (Antes et al. 2001; West et al. 2002) and previously in plants (Singer et al. 2011, 2012). In some cases, orientation-dependence is a consequence of composite elements with both insulator and enhancer activities (Antes et al. 2001; West et al. 2002; Singer et al. 2012). An alternative hypothesis for orientation dependence is that structural properties of the insulator DNA contribute to insulator function. This hypothesis is also consistent with our finding that GC content is a major contributor to insulator activity.

Short insulator elements are useful for plant biotechnology to minimize the size of transgene cassettes to ensure efficient transformation. Transgene cassettes, especially those composed of multiple genes, often show unpredictable expression patterns even when the regulation of the individual genes is well characterized (Kallam et al. 2023). The insulators identified here are promising building blocks to make expression more predictable and thus plant engineering more economically feasible. Recent advances in the construction of synthetic genetic circuits in plants could enable researchers to rationally reprogram plant development, architecture, metabolism, or stress responses (Guiziou et al. 2021; Brophy et al. 2022; Lloyd et al. 2022; Selma et al. 2022; Vazquez-Vilar et al. 2023; Khan et al. 2025). To ensure correct functioning of such synthetic genetic circuits, it is crucial to prevent regulatory crosstalk among the individual circuit units which could be achieved with the insulators identified here.

Insulator activity showed some specificity to the *N. benthamiana* or maize system, suggesting that insulators need to be designed for either dicots or monocots. Although our work shows that the use of insulators in transgene cassettes must account for both their silencer and insulator activities, plant biotechnology efforts tend to use strong constitutive promoters, such that silencer activity is negligible. Moreover, when used with tissue-or condition-specific enhancers, insulators with enhancer-dependent silencer activity could be beneficial. Such insulator-enhancer combinations could repress leaky expression in tissues or conditions in which the enhancer is inactive and insulate expression when the enhancer becomes fully active. Similarly, the dual-function elements identified here might be used to fine-tune transgene expression by repressing overly active transcription while simultaneously isolating the transgene from other surrounding regulatory elements.

Materials and methods

Library design and construction

The full-length λ-EXOB, BEAD-1C, UASrpg, and gypsy insulators were ordered as synthesized DNA fragments from IDT. The synthetic insulators sIns1 and sIns2 were PCR amplified from pZS*11_4enh (Addgene no. 149423; https://www.addgene.org/149423/) (Jores et al. 2020) and pEvolvR-enCas9-PolI3M-TBD (Addgene no. 113077; https://www.addgene.org/113077/) (Halperin et al. 2018), respectively. Insulator fragments were ordered as an oligonucleotide array from Twist Bioscience with 15 bp flanking sequences for amplification. The 35S, *AB80*, and *Cab-1* enhancers were PCR amplified from pZS*11_4enh. The At-9661, Sl-12881, Sb-11289, Zm-23177, and Sl-774 enhancers were ordered as synthesized DNA fragments from Twist Bioscience. The sequences of the full-length insulators and the oligonucleotides used in this study are listed in Supplementary Table S4 and Supplementary Table S5, respectively.

All libraries used in this study were constructed using pPSm, a shortened version of pPSup (Addgene no. 149416; https://www.addgene.org/149416/) (Jores et al. 2020) lacking the BlpR cassette, as the base plasmid. The plasmid's T-DNA region harbors a GFP reporter construct terminated by the poly(A) site of the Arabidopsis (*Arabidopsis thaliana*) ribulose bisphosphate carboxylase small chain 1A gene. Two versions of pPSm were created to receive insulators in the forward (pPSmF) or reverse (pPSmR) orientation by changing the BsaI scars to ACTC and CTGT or ACAG and GAGT, respectively. The plasmids were deposited at Addgene (Addgene no. 226912 and 226913; https://www.addgene.org/226912/; https://www.addgene.org/226913/). Gibson assembly (Gibson et al. 2009) was used to insert enhancers into pPSm plasmids. The 35S minimal promoter (−46 to +5 relative to the 35S transcription start site) followed by the 5′ UTR from a maize histone H3 gene (Zm00001d041672) and an 18-bp random barcode (VNNVNNVNNVNNVNNVNN; V = A, C, or G) downstream of an ATG start codon was cloned in front of the second codon of GFP by Golden Gate cloning (Engler et al. 2008) using BbsI-HF (NEB). To distinguish between sub-libraries, positions 1, 4, 7, 10, 13, and 16 of the barcodes were set to fixed bases. Insulators and insulator fragments were inserted into the pPSm plasmids by Golden Gate cloning using BsaI-HFv2 (NEB). The resulting libraries were bottlenecked to yield about 20 to 50 barcodes per enhancer.

The base plasmid for dual-luciferase constructs was derived from pDL (Addgene no. 208978; https://www.addgene.org/208978/) (Jores et al. 2024) by changing the BsaI scars to ACTC and CTGT. The 35S or *AB80* enhancer was inserted into this plasmid upstream or downstream of the BsaI Golden Gate cassette via Gibson assembly. Full-length insulators and insulator fragments were inserted by Golden Gate cloning using BsaI-HFv2 (NEB). For rice dual-luciferase constructs, the BlpR cassette was replaced by a hygromycin resistance gene under control of the switchgrass polyubiquitin 2 promoter and the 35S terminator derived from plasmid JD633 (Addgene no. 160393; https://www.addgene.org/160393/) (Debernardi et al. 2020).

The expression cassettes for the Agrobacterium-based transformation vectors to generate transgenic corn plants consisted of a reporter gene driven by the constitutive, moderate-strength *ZmGOS2* promoter (Barbour et al. 2003) coupled to a heterologous intron with either the CaMV 35S enhancer upstream of the promoter (negative control) or no enhancer (positive control). The same terminator was used in cassettes to terminate transcription. The insulators were tested using the expression cassette with the 35S enhancer by inserting them between the 35S enhancer and the promoter.

N. benthamiana cultivation and transformation

N. benthamiana was grown in soil (Sunshine Mix no. 4) at 25 °C in a long-day photoperiod (16 h light and 8 h dark; cool-white fluorescent lights [Philips TL-D 58 W/840]; intensity 300 $\mu mol\, m^{-2}\, s^{-1}$). Plants were transformed approximately 3 weeks after germination. For transient transformation of *N. benthamiana* leaves, Plant STARR-seq libraries were introduced into *Agrobacterium tumefaciens* strain GV3101 (harboring the virulence plasmid pMP90 and the helper plasmid pMisoG) by electroporation. An overnight culture of the transformed *A. tumefaciens* was diluted into 100 mL YEP medium (1% [w/v] yeast extract and 2% [w/v] peptone) and grown at 28 °C for 8 h. A 5-mL input sample of the cells was collected, and plasmids were isolated from it using the QIAprep Spin Miniprep Kit (QIAGEN) according to the manufacturer's

instructions. The remaining cells were harvested and resuspended in 100 mL induction medium (M9 medium [3 g/L KH_2PO_4, 0.5 g/L NaCl, 6.8 g/L Na_2HPO_4, and 1 g/L NH_4Cl] supplemented with 1% [w/v] glucose, 10 mM MES, pH 5.2, 100 μM $CaCl_2$, 2 mM $MgSO_4$, and 100 μM acetosyringone). After overnight growth, the *Agrobacteria* were harvested, resuspended in infiltration solution (10 mM MES, pH 5.2, 10 mM $MgCl_2$, 150 μM acetosyringone, and 5 μM lipoic acid) to an optical density (OD) of 1 and infiltrated into leaves 3 and 4 of 2 (full-length insulator library) or 4 (all other libraries) *N. benthamiana* plants. The plants were further grown for 48 h under normal conditions (16 h light and 8 h dark) or in the dark before mRNA extraction.

Maize cultivation and transformation

For Plant STARR-seq in maize (*Zea mays* L. cultivar B73), we used PEG transformation method as previously described (Tonnies et al. 2023). Maize seeds were germinated in soil at 25 °C in a long-day photoperiod (16 h light and 8 h dark; cool-white fluorescent lights [Philips TL-D 58 W/840]; intensity 300 μmol m^{-2} s^{-1}). After 3 days, the seedlings were moved to complete darkness at 25 °C and grown for 10 to 11 days. From each seedling, 10 cm sections from the 2nd and 3rd leaves were cut into thin 0.5 mm strips perpendicular to veins and immediately submerged in 10 mL of protoplasting enzyme solution (0.6 M mannitol, 10 mM MES pH 5.7, 15 mg/mL cellulase R10, 3 mg/mL macerozyme, 1 mM $CaCl_2$, 0.1% [w/v] BSA, and 5 mM beta-mercaptoethanol). The mixture was covered in foil to keep out light, vacuum infiltrated for 3 min, and incubated on a shaker at 40 rpm for 2.5 h. Protoplasts were released by incubating an extra 10 min at 80 rpm. To quench the reaction, 10 mL ice-cold MMG (0.6 M mannitol, 4 mM MES pH 5.7, 15 mM $MgCl_2$) was added to the enzyme solution and the whole solution was filtered through a 40 μM cell strainer. To pellet protoplasts, the filtrate was split into equal volumes of no more than 10 mL in chilled round-bottom glass centrifuge vials and centrifuged at 100 × *g* for 4 min at room temperature (RT). Pellets were resuspended in 1 mL cold MMG each and combined into a single round-bottom vial. To wash, MMG was added to make a total volume of 5 mL and the solution was centrifuged at 100 × *g* for 3 min at RT. This wash step was repeated 2 more times. The final pellet was resuspended in 1 to 2 mL of MMG. A sample of the resuspended protoplasts was diluted 1:20 in MMG and used to count the number of viable cells using fluorescein diacetate as a dye. For each replicate, 1 to 10 million protoplasts were mixed with 15 μg per million protoplasts of the Plant STARR-seq plasmid library in a fresh tube, topped with MMG to a volume of 114.4 μL per million protoplasts, and incubated on ice for 30 min. For PEG transformation, 105.6 μL per million protoplasts of PEG solution (0.6 M Mannitol, 0.1 M $CaCl_2$, 25% [w/v] poly-ethylene glycol MW 4000) was added to reach a final concentration of 12% (w/v) PEG. The mixture was incubated for 10 min in the dark at RT. After incubation, the transformation solution was diluted with 5 volumes of incubation solution (0.6 M Mannitol, 4 mM MES pH 5.7, 4 mM KCl), and centrifuged at 100 × *g* for 4 min at RT. The protoplast pellet was washed with 5 mL of incubation solution, centrifuged at 100 × *g* for 3 min at RT, and resuspended in incubation solution to a concentration of 500 cells/μL. Protoplasts were incubated overnight in the dark at RT to allow for transcription of the plasmid library and then pelleted (4 min, 100 × *g*, RT). The pellet was washed with 1 to 5 mL incubation solution and centrifuged (3 min, 100 × *g*, RT). The pellet was finally resuspended in 1 to 5 mL incubation solution. An aliquot of the solution was used to check transformation efficiency under a microscope. Cells were pelleted (4 min, 100 × *g*, RT) and resuspended in 1 to 2 mL Trizol for subsequent mRNA extraction. An aliquot of the plasmid library used for PEG transformation was used as the input sample for Plant STARR-seq.

To generate stable transgenic maize plants, we followed a previously published procedure (Anand et al. 2019).

Arabidopsis cultivation and transformation

Arabidopsis thaliana Col-0 was grown in soil (Sunshine Mix no. 4) at 20 °C in a long-day photoperiod (16 h light and 8 h dark; cool-white fluorescent lights [Sylvania FO32/841/ECO 32W]; intensity 100 μmol m^{-2} s^{-1}). For transformation, dual-luciferase plasmids were introduced into *Agrobacterium tumefaciens* strain GV3101 (harboring the virulence plasmid pMP90 and the helper plasmid pMisoG) by electroporation. Transgenic Arabidopsis plants were generated by floral dipping (Clough and Bent 1998) and selected for by spraying with a 0.01% (w/v) glufosinate solution.

Rice cultivation and transformation

The rice (*Oryza sativa* L. ssp. *japonica*) cultivar Kitaake was used for genetic transformation following a previously described protocol (Hiei and Komari 2008) with slight modifications. The mature seeds were sterilized with a 7.5% (w/v) sodium hypochlorite solution for 20 min, followed by 3 sterile water rinses. The seeds were placed on callus induction medium (4.4 g/L MS salts with vitamins, 30 g/L sucrose, 2 mg/L 2,4-dichlorophenoxyacetic acid, 8 g/L agar, pH 5.8) to induce callus cells from scutellum for 10 days. The calli were co-cultivated on callus induction medium supplemented with 200 μM of acetosyringone for 3 days with the *Agrobacterium* strain EHA101 (OD = 0.5) carrying individual insulator constructs. The callus cells were transferred to callus induction medium supplemented with 300 mg/L timentin and 50 mg/L hygromycin for 2 rounds of selection. The hygromycin-resistant callus cells of individual lines were transferred to regeneration medium (4.4 g/L MS salts with vitamins, 30 g/L sucrose, 3 mg/L 6-benzylaminopurine, 0.5 mg/L 1-naphthaleneacetic acid, 8 g/L agar, 25 mg/L hygromycin, 150 mg/L timentin, pH 5.8) for about 2 rounds to regenerate shoots. The shoots were transferred to rooting medium (4.4 g/L MS salts with vitamins, 30 g/L sucrose, 25 mg/L hygromycin, 8 g/L agar, pH 5.8) and were grown till healthy roots were produced before transferring to soil. The plantlets were transferred to a plastic box containing topsoil from the research farm at the University of Missouri flooded with water. The plantlets were grown in a greenhouse with a short-day photoperiod (12 h light and 12 h dark) at 28 °C and 24 °C during the day and night, respectively.

Plant STARR-seq

Details for the individual Plant STARR-seq experiments including how many leaves or protoplasts and reverse transcription reactions were used, and the number of sequencing reads are listed in Supplementary Table S6. For all Plant STARR-seq experiments, at least 2 independent biological replicates were performed. Different plants and fresh *Agrobacterium* cultures were used for each biological replicate.

For Plant STARR-seq in *N. benthamiana*, whole leaves were harvested 2 days after infiltration and partitioned into batches of 4 leaves. The leaf batches were frozen in liquid nitrogen, finely ground with mortar and pestle, and immediately resuspended in 10 mL QIAzol (Qiagen). The suspensions were cleared by centrifugation (5 min, 4,000 × *g*, 4 °C). The supernatant was transferred to a 15 mL MaXtract High Density tube (Qiagen) and mixed with

2.5 mL chloroform. After centrifugation (10 min, 1,000 × *g*, 4 °C), the supernatant (approximately 7 mL) was poured into a new tube, and mixed by inversion with 3.5 mL high salt buffer (0.8 M sodium citrate, 1.2 M NaCl) and 3.5 mL isopropanol. The solution was incubated for 15 min at RT to precipitate the RNA and centrifuged (30 min, 4,000 × *g*, 4 °C). The pellet was washed with 10 mL ice-cold 70% ethanol, centrifuged (5 min, 4000 × *g*, 4 °C), and air-dried. The pellet was resuspended in 625 µL of warm (65 °C) nuclease-free water and transferred to a new tube. The solution was supplemented with 70 µL 20X DNase I buffer (1 mM $CaCl_2$, 100 mM Tris pH 7.4), 70 µL 200 mM $MnCl_2$, 5 µL DNase I (Thermo Fisher Scientific), and 1 µL RNaseOUT (Thermo Fisher Scientific). After 1 h incubation at 37 °C, the reaction was stopped with 50 µL 500 mM EDTA. To precipitate the RNA, 375 µL high salt buffer and 375 µL isopropanol were added. After incubation for 15 min at room RT, the RNA was pelleted by centrifugation (20 min, 20,000 × *g*, 4 °C). The pellet was washed with 1 mL ice-cold 70% ethanol, centrifuged (5 min, 20,000 × *g*, 4 °C), air-dried, and resuspended in 50 µL nuclease-free water. All batches of the same sample were pooled, and the solution was supplemented with 0.5 µL RNaseOUT. For cDNA synthesis, 2 to 4 reactions with 11 µL RNA solution, 1 µL 10 µM GFP-specific reverse transcription primer, and 1 µL 10 mM dNTPs were incubated at 65 °C for 5 min then immediately placed on ice. The reactions were supplemented with 4 µL 5X SuperScript IV buffer, 1 µL 100 mM DTT, 1 µL RNaseOUT, and 1 µL SuperScript IV reverse transcriptase (Thermo Fisher Scientific). To ensure that the samples were largely free of DNA contamination, 2 to 4 additional reactions were used as controls, where the reverse transcriptase and RNaseOUT were replaced with water. Reactions were incubated for 10 min at 55 °C, followed by 10 min at 80 °C. Sets of 4 reactions each were pooled. The cNDA was purified with the Clean&Concentrate-5 kit (Zymo Research), and eluted in 20 µL 10 mM Tris. The barcode was amplified with 10 to 20 cycles of polymerase chain reaction (PCR) and read out by next-generation sequencing.

For Plant STARR-seq in maize protoplasts, the protoplast-containing Trizol solution from PEG transformation was transferred to 2 mL Phasemaker tubes (1 mL per tube; Thermo Fisher Scientific), mixed thoroughly with 300 µL chloroform, and centrifuged (5 min, 15,000 × *g*, 4 °C). RNA was extracted using the RNeasy Plant Mini Kit (QIAGEN). The supernatant was transferred to a QIAshredder column and centrifuged (2 min, 20,000 × *g*, RT). The flowthrough was transferred to a new 1.5 mL tube and mixed with 300 µL 100% ethanol. Up to 500 µL of the solution was loaded on an RNeasy mini spin column. After centrifugation (10 s, 16,100 × *g*, RT) the flowthrough was discarded. This was repeated until the whole solution had been added to the column. The column was washed with 350 µL RW1 buffer followed by centrifugation (30 s, 16,100 × *g*, RT). An on-column DNase I digestion was performed with 70 µL RDD buffer and 10 µL DNase I (Qiagen) for 15 min at RT. The column was washed once with 350 µL RW1 buffer and twice with 500 µL RPE buffer. After each wash step, the column was centrifuged (30 s, 16,100 × *g*, RT) and the flowthrough was discarded. The column was dried with an extra centrifugation step (30 s, 16,100 × *g*, RT) and transferred to a 1.5 mL collection tube. For elution, 50 µL of RNase-free water was added, and the column was incubated for 1 min, and centrifuged (1 min, 16,100 × *g*, RT). This elution step was repeated with an additional 40 µL of RNase-free water. The eluate was treated with DNase I (5 µL of 20x DNaseI buffer, 5 µL 200 mM $MnCl_2$, 1 µL RNaseOUT, and 2 µL DNase I) for 1 h at 37 °C. The solution was supplemented with 20 µL 500 mM EDTA, 1 µL 20 mg/mL glycogen, 12 µL ice-cold 8 M LiCl, and 300 µL ice-cold 100% ethanol. The solution was incubated 15 min at −80 °C, centrifuged (20 min, 20,000 × *g*, 4 °C). The pellet was washed with 500 µL ice-cold 70% ethanol and centrifuged (3 min, 20,000 × *g*, 4 °C). The pellet was air-dried and resuspended in 100 µL RNase-free water. Reverse transcription, purification, PCR amplification, and sequencing were performed as for the *N. benthamiana* samples.

Subassembly and barcode sequencing

All sequencing was performed on an Illumina NextSeq 550 or 2000 system. To link insulator fragments to their respective barcodes, the insulator region was sequenced using paired-end reads (100 to 150 bp), and 2 18-bp indexing reads were used to sequence the barcodes. For each Plant STARR-seq experiment, barcodes were sequenced using 18-bp paired-end reads. Paired reads were assembled using PANDAseq (version 2.11) (Masella et al. 2012). Insulator fragment-barcode pairs with less than 5 reads and insulator fragments with a mutation or truncation were discarded.

Computational methods

For analysis of the Plant STARR-seq experiments, the reads for each barcode were counted in the input and cDNA samples. Barcode counts below 5 were discarded. Barcode counts were normalized to the sum of all counts in the respective sample. For barcodes, enrichment was calculated by dividing the normalized barcode counts in the cDNA sample by that in the corresponding input sample. The sum of the normalized counts for all barcodes associated with a given insulator or insulator fragment was used to calculate its enrichment. For each replicate, the enrichment was normalized to the median enrichment. The mean enrichment across all replicates was normalized to the control construct with enhancer or insulator (noEnh) and used for all analyses. Spearman and Pearson's correlation were calculated using base R (version 4.3.1). Linear regression analysis was performed using the lm() function in base R with default parameters (e.g. lm($y \sim x$)). The base R function t.test() was used to calculate 95% confidence intervals.

To predict the enrichment of insulator fragment combinations, a linear model was fitted to Plant STARR-seq data using the lm() function in R with the formula: log2(insulator activity) = log2(insulator activity fragment 3) + log2(insulator activity fragment 2) + log2(insulator activity fragment 1), where log2(insulator activity fragment 1 to 3) is the enhancer strength of the corresponding fragment when tested individually. Fragments are numbered by increasing distance from the minimal promoter (fragment 1 is the fragment closest to the promoter, fragment 3 the most distal 1). Insulator activity was calculated with: log2(insulator activity) = log2(enrichment noIns control) − log2(enrichment insulator). For constructs with 1 or 2 fragments, log2(insulator activity) was set to 0 for fragments 3 (2-fragment constructs) or 2 and 3 (1-fragment constructs).

Dual-luciferase assay

Transgenic Arabidopsis lines (T2 generation) with dual-luciferase constructs were grown in soil for 3 weeks. A cork borer (4 mm diameter) was used to collect a total of 4 leaf discs from the 3rd and 4th leaves of the plants. The leaf discs were transferred to 1.5 mL tubes filled with approximately 10 glass beads (1 mm diameter), snap-frozen in liquid nitrogen, and disrupted by shaking twice for 5 s in a Silamat S6 (Ivoclar) homogenizer. The leaf disc debris was resuspended in 100 µL 1X Passive Lysis Buffer (Promega). The solution was cleared by centrifugation (5 min, 20,000 × *g*, RT) and 10 µL of the supernatant were mixed with 90 µL 1X passive lysis buffer. Luciferase and nanoluciferase activity were

measured on a Biotek Synergy H1 plate reader using the Promega Nano-Glo Dual-Luciferase Reporter Assay System according to the manufacturer's instructions. Specifically, 10 μL of the leaf extracts were combined with 75 μL ONE-Glo EX Reagent, mixed for 3 min at 425 rpm, and incubated for 2 min before measuring luciferase activity. Subsequently, 75 μL NanoDLR Stop&Glo Reagent were added to the sample. After 3 min mixing at 425 rpm and 12 min incubation, nanoluciferase activity was measured. Two independent biological replicates were performed.

For transgenic rice lines with dual-luciferase constructs, 10 to 15 mg leaf tissue from a 3-week old T0 plants was collected in 1.5 mL tubes filled with approximately 10 glass beads (1 mm diameter). The material was snap-frozen in liquid nitrogen and disrupted by shaking twice for 5 s in a Silamat S6 (Ivoclar) homogenizer. The leaf debris was resuspended in 200 μL 1X Passive Lysis Buffer (Promega). The solution was cleared by centrifugation (5 min, 20,000 × *g*, RT) and 10 μL of the supernatant were mixed with 90 μL 1X passive lysis buffer. Luciferase and nanoluciferase activity were measured on a Biotek Synergy H1 in the same way as for Arabidopsis samples. Two independent technical replicates (using new samples from the same plants as in the first replicate) were performed.

ELISA

Insulator activity was detected using a quantitative ELISA on leaf, stalk, silk, and husk tissues collected from transgenic corn plants. Tissue samples were extracted with 0.60 to 2.5 mL of buffer comprised of phosphate buffered saline containing polysorbate 20 (8.10 mM PBS + 0.05% polysorbate). Extracted samples were centrifuged and the supernatants were used for analysis. 96-well plates precoated with reporter-specific monoclonal antibody were incubated with standards and the samples (1 h). After incubation and washing, a second reporter-specific monoclonal antibody, conjugated to a horseradish peroxidase enzyme (HRP) was added to the plate and incubated (1 h). After incubation, the plates were washed 5 times and the bound protein-antibody complex was detected by adding TMB (3,3′,5,5′-tetramethylbenzidine) substrate which generated a colored product in the presence of HRP. The reaction was stopped by adding an acid solution and the OD of each well was determined using a plate reader at 450 nm. For each plate, a standard curve was included. Adjusted sample concentration values were converted from ng mL^{-1} to ng mg^{-1} total extractable protein.

Accession numbers

The code used for the analysis and to generate the figures is available on GitHub (https://github.com/tobjores/Small-DNA-elements-can-act-as-both-insulators-and-silencers-in-plants). All barcode sequencing reads were deposited in the National Center for Biotechnology Information (NCBI) Sequence Read Archive under the BioProject accession PRJNA1160710 (http://www.ncbi.nlm.nih.gov/bioproject/1160710/).

Acknowledgments

We acknowledge Scott Betts, Hyeon-Je Cho, Megan Christenson, Terry Hu, Albert Lu, Leanne Thompson, Kelli Van Waus, Ning Wang, and Emily Wu for their contributions to the work.

Author contributions

All authors conceived and interpreted experiments; T.J., N.A.M., J.T., S.N.C., B.L., V.G.-A., and S.J. performed experiments; T.J. analyzed the data and prepared figures; T.J., N.A.M., S.F., and C.Q. wrote the manuscript. All authors read and revised the manuscript.

Supplementary data

The following materials are available in the online version of this article.

Supplementary Figure S1. Plant STARR-seq detects activity of enhancer-blocking insulators.

Supplementary Figure S2. Plant STARR-seq yields highly reproducible results.

Supplementary Figure S3. Activity of insulator fragments in different maize tissues.

Supplementary Figure S4. Activity of insulator fragment combinations in different maize tissues.

Supplementary Figure S5. Enhancers downstream of insulator fragments slightly reduce their activity.

Supplementary Figure S6. Enhancer-dependent silencer activity in stable transgenic plants.

Supplementary Table S1. Insulator fragments used in fragment combination library.

Supplementary Table S2. Insulator fragment combinations tested in stable transgenic maize lines.

Supplementary Table S3. Insulators and insulator fragments used in the enhancer–insulator combination library.

Supplementary Table S4. Full-length insulator sequences.

Supplementary Table S5. Oligonucleotides used in this study.

Supplementary Table S6. Experimental details for Plant STARR-seq experiments.

Supplementary Data Set 1. Enrichment of insulator fragment constructs.

Supplementary Data Set 2. Enrichment of insulator fragment combination constructs.

Supplementary Data Set 3. Enrichment of insulator fragment constructs with a downstream enhancer.

Supplementary Data Set 4. Enrichment of insulator fragments in insulator and silencer constructs.

Supplementary Data Set 5. Enrichment of insulator and silencer constructs with 8 different enhancers.

Funding

This work was supported by the U.S. National Science Foundation (RESEARCH-PGR grant no. 1748843 to S.F. and C.Q. and PlantSynBio grant no. 2240888 to C.Q.), the German Research Foundation (DFG; postdoctoral fellowship no. 441540116 to T.J., Emmy Noether program grant no. 517938232 to T.J., and Germany's Excellence Strategy—EXC-2048/1—project ID 390686111 to T.J.), the National Institutes of Health (T32 training grant no. HG000035 to J.T., NIGMS grant no. R01-GM079712 to J.T.C. and C.Q., and NIGMS MIRA grant no. 1R35GM139532 to C.Q.), and the United States Department of Agriculture (NIFA postdoctoral fellowship no. 2023-67012-39445 to N.A.M.).

Conflict of interest statement. T.J., J.T.C., and C.Q. have filed a patent application related to this work through the University of Washington. The remaining authors declare no competing interests.

Data availability

The raw sequencing data underlying this article are available in the National Center for Biotechnology Information (NCBI) Sequence

Read Archive at http://www.ncbi.nlm.nih.gov/bioproject/1160710. The processed data underlying this article are available on GitHub at https://github.com/tobjores/Small-DNA-elements-can-act-as-both-insulators-and-silencers-in-plants.

References

Anand A, Wu E, Li Z, TeRonde S, Arling M, Lenderts B, Mutti JS, Gordon-Kamm W, Jones TJ, Chilcoat ND. High efficiency Agrobacterium-mediated site-specific gene integration in maize utilizing the FLP-FRT recombination system. *Plant Biotechnol J*. 2019:17(8):1636–1645. https://doi.org/10.1111/pbi.13089

Antes TJ, Namciu SJ, Fournier REK, Levy-Wilson B. The 5′ boundary of the human apolipoprotein B chromatin domain in intestinal cells. *Biochemistry*. 2001:40(23):6731–6742. https://doi.org/10.1021/bi0100743

Banerji J, Rusconi S, Schaffner W. Expression of a β-globin gene is enhanced by remote SV40 DNA sequences. *Cell*. 1981:27(2 Pt 1):299–308. https://doi.org/10.1016/0092-8674(81)90413-X

Barbour E, Meyer TE, Saad ME. Maize Gos-2 promoters. Patent US 6.504.083. 2003.

Bell AC, West AG, Felsenfeld G. The protein CTCF is required for the enhancer blocking activity of vertebrate insulators. *Cell*. 1999:98(3):387–396. https://doi.org/10.1016/S0092-8674(00)81967-4

Brophy JAN, Magallon KJ, Duan L, Zhong V, Ramachandran P, Kniazev K, Dinneny JR. Synthetic genetic circuits as a means of reprogramming plant roots. *Science*. 2022:377(6607):747–751. https://doi.org/10.1126/science.abo4326

Burgess-Beusse B, Farrell C, Gaszner M, Litt M, Mutskov V, Recillas-Targa F, Simpson M, West A, Felsenfeld G. The insulation of genes from external enhancers and silencing chromatin. *Proc Natl Acad Sci U S A*. 2002:99(Suppl 4):16433–16437. https://doi.org/10.1073/pnas.162342499

Chetverina D, Aoki T, Erokhin M, Georgiev P, Schedl P. Making connections: insulators organize eukaryotic chromosomes into independent cis-regulatory networks. *BioEssays*. 2014:36(2):163–172. https://doi.org/10.1002/bies.201300125

Clough SJ, Bent AF. Floral dip: a simplified method for *Agrobacterium*-mediated transformation of *Arabidopsis thaliana*. *Plant J*. 1998:16(6):735–743. https://doi.org/10.1046/j.1365-313x.1998.00343.x

Cuperus JT. Single-cell genomics in plants: current state, future directions, and hurdles to overcome. *Plant Physiol*. 2022:188(2):749–755. https://doi.org/10.1093/plphys/kiab478

Debernardi JM, Tricoli DM, Ercoli MF, Hayta S, Ronald P, Palatnik JF, Dubcovsky J. A GRF–GIF chimeric protein improves the regeneration efficiency of transgenic plants. *Nat Biotechnol*. 2020:38(11):1274–1279. https://doi.org/10.1038/s41587-020-0703-0

Engler C, Kandzia R, Marillonnet S. A one pot, one step, precision cloning method with high throughput capability. *PLoS One*. 2008:3(11):e3647. https://doi.org/10.1371/journal.pone.0003647

Gaszner M, Felsenfeld G. Insulators: exploiting transcriptional and epigenetic mechanisms. *Nat Rev Genet*. 2006:7(9):703–713. https://doi.org/10.1038/nrg1925

Gaszner M, Vazquez J, Schedl P. The Zw5 protein, a component of the scs chromatin domain boundary, is able to block enhancer–promoter interaction. *Genes Dev*. 1999:13(16):2098–2107. https://doi.org/10.1101/gad.13.16.2098

Gdula DA, Gerasimova TI, Corces VG. Genetic and molecular analysis of the gypsy chromatin insulator of Drosophila. *Proc Natl Acad Sci U S A*. 1996:93(18):9378–9383. https://doi.org/10.1073/pnas.93.18.9378

Gibson DG, Young L, Chuang R-Y, Venter JC, Hutchison CA 3rd, Smith HO. Enzymatic assembly of DNA molecules up to several hundred kilobases. *Nat Methods*. 2009:6(5):343–345. https://doi.org/10.1038/nmeth.1318

Gisselbrecht SS, Palagi A, Kurland JV, Rogers JM, Ozadam H, Zhan Y, Dekker J, Bulyk ML. Transcriptional silencers in *Drosophila* serve a dual role as transcriptional enhancers in alternate cellular contexts. *Mol Cell*. 2020:77(2):324–337.e8. https://doi.org/10.1016/j.molcel.2019.10.004

Gorjifard S, Jores T, Tonnies J, Mueth NA, Bubb K, Wrightsman T, Buckler ES, Fields S, Cuperus JT, Queitsch C. Arabidopsis and maize terminator strength is determined by GC content, polyadenylation motifs and cleavage probability. *Nat Commun*. 2024:15(1):5868. https://doi.org/10.1038/s41467-024-50174-7

Gudynaite-Savitch L, Johnson DA, Miki BLA. Strategies to mitigate transgene–promoter interactions. *Plant Biotechnol J*. 2009:7(5):472–485. https://doi.org/10.1111/j.1467-7652.2009.00416.x

Guiziou S, Chu JC, Nemhauser JL. Decoding and recoding plant development. *Plant Physiol*. 2021:187(2):515–526. https://doi.org/10.1093/plphys/kiab336

Halperin SO, Tou CJ, Wong EB, Modavi C, Schaffer DV, Dueber JE. CRISPR-guided DNA polymerases enable diversification of all nucleotides in a tunable window. *Nature*. 2018:560(7717):248–252. https://doi.org/10.1038/s41586-018-0384-8

Heger P, Wiehe T. New tools in the box: an evolutionary synopsis of chromatin insulators. *Trends Genet*. 2014:30(5):161–171. https://doi.org/10.1016/j.tig.2014.03.004

Hiei Y, Komari T. Agrobacterium-mediated transformation of rice using immature embryos or calli induced from mature seed. *Nat Protoc*. 2008:3(5):824–834. https://doi.org/10.1038/nprot.2008.46

Hily J-M, Singer SD, Yang Y, Liu Z. A transformation booster sequence (TBS) from Petunia hybrida functions as an enhancer-blocking insulator in *Arabidopsis thaliana*. *Plant Cell Rep*. 2009:28(7):1095–1104. https://doi.org/10.1007/s00299-009-0700-8

Jores T, Hamm M, Cuperus JT, Queitsch C. Frontiers and techniques in plant gene regulation. *Curr Opin Plant Biol*. 2023:75:102403. https://doi.org/10.1016/j.pbi.2023.102403

Jores T, Tonnies J, Dorrity MW, Cuperus JT, Fields S, Queitsch C. Identification of plant enhancers and their constituent elements by STARR-seq in tobacco leaves. *Plant Cell*. 2020:32(7):2120–2131. https://doi.org/10.1105/tpc.20.00155

Jores T, Tonnies J, Mueth NA, Romanowski A, Fields S, Cuperus JT, Queitsch C. Plant enhancers exhibit both cooperative and additive interactions among their functional elements. *Plant Cell*. 2024:36(7):2570–2586. https://doi.org/10.1093/plcell/koae088

Jores T, Tonnies J, Wrightsman T, Buckler ES, Cuperus JT, Fields S, Queitsch C. Synthetic promoter designs enabled by a comprehensive analysis of plant core promoters. *Nat Plants*. 2021:7(6):842–855. https://doi.org/10.1038/s41477-021-00932-y

Kallam K, Moreno-Giménez E, Mateos-Fernández R, Tansley C, Gianoglio S, Orzaez D, Patron N. Tunable control of insect pheromone biosynthesis in *Nicotiana benthamiana*. *Plant Biotechnol J*. 2023:21(7):1440–1453. https://doi.org/10.1111/pbi.14048

Khan MA, Herring G, Zhu JY, Oliva M, Fourie E, Johnston B, Zhang Z, Potter J, Pineda L, Pflueger J, et al. CRISPRi-based circuits to control gene expression in plants. *Nat Biotechnol*. 2025:43(3):416–430. https://doi.org/10.1038/s41587-024-02236-w

Kurbidaeva A, Purugganan M. Insulators in plants: progress and open questions. *Genes (Basel)*. 2021:12(9):1422. https://doi.org/10.3390/genes12091422

Laimins L, Holmgren-König M, Khoury G. Transcriptional "silencer" element in rat repetitive sequences associated with the rat

insulin 1 gene locus. *Proc Natl Acad Sci U S A*. 1986:83(10): 3151–3155. https://doi.org/10.1073/pnas.83.10.3151

Lloyd JPB, Ly F, Gong P, Pflueger J, Swain T, Pflueger C, Fourie E, Khan MA, Kidd BN, Lister R. Synthetic memory circuits for stable cell reprogramming in plants. *Nat Biotechnol*. 2022:40(12):1862–1872. https://doi.org/10.1038/s41587-022-01383-2

Masella AP, Bartram AK, Truszkowski JM, Brown DG, Neufeld JD. PANDAseq: paired-end assembler for illumina sequences. *BMC Bioinformatics*. 2012:13(1):31. https://doi.org/10.1186/1471-2105-13-31

Ogbourne S, Antalis TM. Transcriptional control and the role of silencers in transcriptional regulation in eukaryotes. *Biochem J*. 1998:331(Pt 1):1–14. https://doi.org/10.1042/bj3310001

Pang B, Snyder MP. Systematic identification of silencers in human cells. *Nat Genet*. 2020:52(3):254–263. https://doi.org/10.1038/s41588-020-0578-5

Parkhurst SM, Harrison DA, Remington MP, Spana C, Kelley RL, Coyne RS, Corces VG. The Drosophila su(Hw) gene, which controls the phenotypic effect of the gypsy transposable element, encodes a putative DNA-binding protein. *Genes Dev*. 1988:2(10): 1205–1215. https://doi.org/10.1101/gad.2.10.1205

Recillas-Targa F, Pikaart MJ, Burgess-Beusse B, Bell AC, Litt MD, West AG, Gaszner M, Felsenfeld G. Position-effect protection and enhancer blocking by the chicken β-globin insulator are separable activities. *Proc Natl Acad Sci U S A*. 2002:99(10):6883–6888. https://doi.org/10.1073/pnas.102179399

Ricci WA, Lu Z, Ji L, Marand AP, Ethridge CL, Murphy NG, Noshay JM, Galli M, Mejía-Guerra MK, Colomé-Tatché M, et al. Widespread long-range cis-regulatory elements in the maize genome. *Nat Plants*. 2019:5(12):1237–1249. https://doi.org/10.1038/s41477-019-0547-0

Schmitz RJ, Grotewold E, Stam M. Cis-regulatory sequences in plants: their importance, discovery, and future challenges. *Plant Cell*. 2022:34(2):718–741. https://doi.org/10.1093/plcell/koab281

Selma S, Sanmartín N, Espinosa-Ruiz A, Gianoglio S, Lopez-Gresa MP, Vázquez-Vilar M, Flors V, Granell A, Orzaez D. Custom-made design of metabolite composition in *N. benthamiana* leaves using CRISPR activators. *Plant Biotechnol J*. 2022:20(8):1578–1590. https://doi.org/10.1111/pbi.13834

She W, Lin W, Zhu Y, Chen Y, Jin W, Yang Y, Han N, Bian H, Zhu M, Wang J. The gypsy insulator of *Drosophila melanogaster*, together with its binding protein suppressor of hairy-wing, facilitate high and precise expression of transgenes in *Arabidopsis thaliana*. *Genetics*. 2010:185(4):1141–1150. https://doi.org/10.1534/genetics.110.117960

Singer SD, Cox KD. A gypsy-like sequence from *Arabidopsis thaliana* exhibits enhancer-blocking activity in transgenic plants. *J Plant Biochem Biotechnol*. 2013:22(1):35–42. https://doi.org/10.1007/s13562-012-0108-3

Singer SD, Hily J-M, Cox KD. Analysis of the enhancer-blocking function of the TBS element from Petunia hybrida in transgenic *Arabidopsis thaliana* and *Nicotiana tabacum*. *Plant Cell Rep*. 2011:30(11):2013–2025. https://doi.org/10.1007/s00299-011-1109-8

Singer SD, Hily J-M, Liu Z. A 1-kb bacteriophage lambda fragment functions as an insulator to effectively block enhancer–promoter interactions in *Arabidopsis thaliana*. *Plant Mol Biol Report*. 2009:28(1):69–76. https://doi.org/10.1007/s11105-009-0122-3

Singer SD, Liu Z, Cox KD. Minimizing the unpredictability of transgene expression in plants: the role of genetic insulators. *Plant Cell Rep*. 2012:31(1):13–25. https://doi.org/10.1007/s00299-011-1167-y

Tonnies J, Mueth NA, Gorjifard S, Chu J, Queitsch C. Scalable transfection of maize mesophyll protoplasts. *J Vis Exp*. 2023:196: e64991. https://doi.org/10.3791/64991

van der Geest AHM, Hall TC. The β-phaseolin 5′ matrix attachment region acts as an enhancer facilitator. *Plant Mol Biol*. 1997:33(3): 553–557. https://doi.org/10.1023/A:1005765525436

Vazquez-Vilar M, Selma S, Orzaez D. The design of synthetic gene circuits in plants: new components, old challenges. *J Exp Bot*. 2023:74(13):3791–3805. https://doi.org/10.1093/jxb/erad167

Vogelmann J, Valeri A, Guillou E, Cuvier O, Nollmann M. Roles of chromatin insulator proteins in higher-order chromatin organization and transcription regulation. *Nucleus*. 2011:2(5):358–369. https://doi.org/10.4161/nucl.2.5.17860

Voichek Y, Hristova G, Mollá-Morales A, Weigel D, Nordborg M. Widespread position-dependent transcriptional regulatory sequences in plants. *Nat Genet*. 2024:56(10):2238–2246. https://doi.org/10.1038/s41588-024-01907-3

Weising K, Kahl G. Towards an understanding of plant gene regulation: the action of nuclear factors. *Z. Für Naturforschung C*. 1991:46(1–2):1–11. https://doi.org/10.1515/znc-1991-1-202

West AG, Gaszner M, Felsenfeld G. Insulators: many functions, many mechanisms. *Genes Dev*. 2002:16(3):271–288. https://doi.org/10.1101/gad.954702

Zhao K, Hart CM, Laemmli UK. Visualization of chromosomal domains with boundary element-associated factor BEAF-32. *Cell*. 1995:81(6):879–889. https://doi.org/10.1016/0092-8674(95)90008-X